

平成28年 3月 2日
千葉大学 大学院理学研究科

がん細胞を死滅させ、かつ、がん免疫を活性化する 夢の化合物を発見

本研究は、千葉大学（学長：徳久剛史）大学院理学研究科基盤理学専攻 坂根郁夫教授を中心とした共同研究チームにより実行された。研究チームは、「がん細胞を死滅させ、かつ、がん免疫を活性化する夢の化合物」を世界で初めて発見した。本化合物を元にがん治療のパラダイムを変える理想の抗癌剤の開発に繋がる可能性がある。

従来の抗がん剤である化学療法剤は、あらゆる細胞に発現している細胞増殖機構を制御するため、正常細胞の増殖も抑制する。特に、骨髄細胞の分化増殖能を低下させ免疫系の不全をもたらすことが臨床において問題となる。近年増加している分子標的治療薬も、その薬物の標的蛋白は正常細胞においても発現しているため、臨床では特有の副作用が生じることが知られている。

ジアシルグリセロールキナーゼ(DGK)の α アイソザイム(DGK α)は悪性黒色腫や肝細胞がんの増殖を亢進するが、Tリンパ球では逆に増殖停止・不活性化(anergy)へ誘導する。従って、DGK α を阻害する薬剤は、直接がん細胞死を誘導し、かつ、Tリンパ球を活性化することでがん免疫亢進作用によるがん細胞死滅が期待でき、理想的・画期的な抗がん剤となると考えられる。そこで、DGK α 阻害化合物を、最近開発したハイスループットスクリーニング系を用い、東京大学創薬機構の化合物ライブラリーをスクリーニングしてDGK α を特異的に阻害する化合物を得た(参考資料1)。本化合物は実際にごん細胞の死滅を誘導し、Tリンパ球を活性化した(参考資料1)。今後更に最適化研究を行い、画期的な次世代抗がん剤の早期開発を目指す。

[参考資料]

1) Liu, K., *et al.* A novel diacylglycerol kinase α -selective inhibitor, CU-3, induces cancer cell apoptosis and enhances immune response. *J. Lipid Res.* 57, 368-379 (2016)

本件に関するお問い合わせ先
千葉大学大学院理学研究科
Tel : 043-290-3695 Fax : 043-290-3695
E-mail : sakane@faculty.chiba-u.jp

A novel diacylglycerol kinase α -selective inhibitor, CU-3, induces cancer cell apoptosis and enhances immune response^S

Ke Liu,* Naoko Kunii,* Megumi Sakuma,[†] Atsumi Yamaki,* Satoru Mizuno,* Mayu Sato,* Hiromichi Sakai,* Sayaka Kado,[§] Kazuo Kumagai,** Hirotatsu Kojima,** Takayoshi Okabe,** Tetsuo Nagano,** Yasuhito Shirai,[†] and Fumio Sakane^{1,*}

Department of Chemistry,* Graduate School of Science and Center for Analytical Instrumentation,[§] Chiba University, Chiba 263-8522, Japan; Department of Applied Chemistry in Bioscience,[†] Graduate School of Agricultural Science, Kobe University, Kobe 657-8501, Japan; and Drug Discovery Initiative,** University of Tokyo, Tokyo 113-0033, Japan

Abstract Diacylglycerol kinase (DGK) consists of 10 isozymes. The α -isozyme enhances the proliferation of cancer cells. However, DGK α facilitates the nonresponsive state of immunity known as T-cell anergy; therefore, DGK α enhances malignant traits and suppresses immune surveillance. The aim of this study was to identify a novel small molecule that selectively and potently inhibits DGK α activity. We screened a library containing 9,600 chemical compounds using a newly established high-throughput DGK assay. As a result, we have obtained a promising compound, 5-[(2E)-3-(2-furyl)prop-2-enylidene]-3-[(phenylsulfonyl)amino]2-thioxo-1,3-thiazolidin-4-one (CU-3), which selectively inhibited DGK α with an IC₅₀ value of 0.6 μ M. CU-3 targeted the catalytic region, but not the regulatory region, of DGK α . CU-3 competitively reduced the affinity of DGK α for ATP, but not diacylglycerol or phosphatidylserine. Moreover, this compound induced apoptosis in HepG2 hepatocellular carcinoma and HeLa cervical cancer cells while simultaneously enhancing the interleukin-2 production of Jurkat T cells. Taken together, these results indicate that CU-3 is a selective and potent inhibitor for DGK α and can be an ideal anticancer drug candidate that attenuates cancer cell proliferation and simultaneously enhances immune responses including anticancer immunity.—Liu, K., N. Kunii, M. Sakuma, A.

Yamaki, S. Mizuno, M. Sato, H. Sakai, S. Kado, K. Kumagai, H. Kojima, T. Okabe, T. Nagano, Y. Shirai, and F. Sakane. **A novel diacylglycerol kinase α -selective inhibitor, CU-3, induces cancer cell apoptosis and enhances immune response.** *J. Lipid Res.* 2016. 57: 368–379.

Supplementary key words cancer • apoptosis • phosphatidic acid • lipid kinases • anergy • T cell • interleukin-2 • high-throughput screening • anticancer drug

Diacylglycerol kinase (DGK) phosphorylates diacylglycerol (DG) to generate phosphatidic acid (1–6). To date, 10 mammalian DGK isozymes (α , β , γ , δ , ϵ , ζ , η , θ , ι , and κ) have been identified. These DGK isozymes are divided into five groups (type I–V) according to their structural features (1–6). Type I DGK isozymes (DGKs α , β , and γ) commonly contain tandem repeats of two EF-hand motif domains and are classified as members of the EF-hand family of Ca²⁺ binding proteins. In addition to the Ca²⁺ binding EF-hand motifs, all type I DGK isozymes contain an N-terminal recoverin homology domain, two cysteine-rich C1 domains, and the C-terminal catalytic region (1–6).

DGK α (7, 8) is highly expressed in hepatocellular carcinoma and melanoma cells (9, 10). DGK α expression is involved in hepatocellular carcinoma progression and is a

This work was supported by Platform for Drug Discovery, Informatics, and Structural Life Science from the Ministry of Education, Culture, Sports, Science and Technology (MEXT), Japan. This work was also supported by MEXT/JSPS KAKENHI Grant Numbers 22370047 [Grant-in-Aid for Scientific Research (B)], 23116505 (Grant-in-Aid for Scientific Research on Innovative Areas), 25116704 (Grant-in-Aid for Scientific Research on Innovative Areas), 26291017 [Grant-in-Aid for Scientific Research (B)], and 15K14470 (Grant-in-Aid for Challenging Exploratory Research); the Japan Science and Technology Agency (AS221Z00794F, AS231Z00139G, AS251Z01788Q, and AS2621643Q), the Naito Foundation, the Hamaguchi Foundation for the Advancement of Biochemistry, the Daiichi-Sankyo Foundation of Life Science, the Terumo Life Science Foundation, the Futaba Electronic Memorial Foundation, the Daiwa Securities Health Foundation, the Ono Medical Research Foundation, the Japan Foundation for Applied Enzymology, the Food Science Institute Foundation, the Skylark Food Science Institute, and the Venture Business Laboratory of Chiba University (F.S.). The authors declare that they have no conflicts of interest to disclose.

Manuscript received 18 August 2015 and in revised form 14 January 2016.

Published, JLR Papers in Press, January 14, 2016
DOI 10.1194/jlr.M062794

Abbreviations: Con A, concanavalin A; CU-3, 5-[(2E)-3-(2-furyl)prop-2-enylidene]-3-[(phenylsulfonyl)amino]2-thioxo-1,3-thiazolidin-4-one; DG, diacylglycerol; DGK, diacylglycerol kinase; HTS, high-throughput screening; IL-2, interleukin-2; PA, phosphatidic acid; PS, phosphatidylserine; R59022, 6-(2-[4-[(4-fluorophenyl)phenylmethylene]1-piperidinyl]ethyl)-7-methyl-5H-thiazolo-(3,2-a)pyrimidin-5-one; R59949, 3-(2-[4-[bis-(4-fluorophenyl)methylene]1-piperidinyl]ethyl)-2,3-dihydro-2-thioxo-4(1H)quinazolinone.

¹To whom correspondence should be addressed.

e-mail: sakane@faculty.chiba-u.jp

^SThe online version of this article (available at <http://www.jlr.org>) contains a supplement.

positive regulator of the proliferative activity of hepatocellular carcinoma through the Ras/Raf/MEK (mitogen-activated protein kinase/ERK kinase)/ERK pathway (9). In melanoma cells, DGK α positively regulates the tumor necrosis factor- α -dependent nuclear factor- κ B (p65) activation via the protein kinase C ζ -mediated Ser311 phosphorylation of p65 (11). Therefore, the suppression of DGK α activity is expected to inhibit the progression of these cancers. On the other hand, DGK α is abundantly expressed in T lymphocytes where it facilitates the nonresponsive state known as anergy (12, 13). Anergy induction in T cells represents the main mechanism for advanced tumors to avoid immune action.

As described above, DGK α has antiapoptosis and proliferation activities in cancer cells (9, 10) and also induces T-cell anergy (12, 13). Therefore, if a DGK α -selective inhibitor is identified and developed, it would reversely attenuate cancer cell proliferation and simultaneously activate T-cell function. There are two commercially available DGK inhibitors, 6-(2-[4-(4-fluorophenyl)phenylmethylene]1-piperidinyl)ethyl)-7-methyl-5*H*-thiazolo-(3,2-*a*)pyrimidin-5-one (R59022) (14, 15) and 3-(2-[4-[bis-(4-fluorophenyl)methylene]1-piperidinyl)ethyl]-2,3-dihydro-2-thioxo-4(1*H*)quinazolinone (R59949) (16, 17); however, we found that R59022 and R59949 only semiselectively inhibited type I, III, and V DGKs α , ϵ , and θ , and type I and II DGKs α , γ , δ , and κ , respectively (18). Moreover, the IC₅₀ values of R59022 and R59949 were \sim 25 μ M and 18 μ M, respectively (18). Therefore, R59022 and R59949 are low selective and low effective inhibitors of DGK α .

To develop highly effective and DGK α -selective inhibitors, a system for high-throughput screening (HTS) is required; however, the conventional DGK assay is quite laborious and requires technical skill. For example, the conventional assay requires the use of a radioisotope ($[\gamma$ -³²P]ATP) and the manipulation of thin-layer chromatography with multiple extraction steps. We recently established a simple DGK assay (18) that is useful for constructing an HTS system for detecting DGK inhibitors from chemical compound libraries.

In this study, we screened a library containing 9,600 chemical compounds to find DGK α -specific inhibitors using the newly established DGK assay for HTS (18). As a result, we have obtained a promising compound, 5-[(2*E*)-3-(2-furyl)prop-2-enylidene]-3-[(phenylsulfonyl)amino]2-thioxo-1,3-thiazolidin-4-one (CU-3), which selectively inhibited DGK α with an IC₅₀ value of 0.6 μ M. Moreover, CU-3 simultaneously enhanced the apoptosis of cancer cells and the activation of T cells.

MATERIALS AND METHODS

Cell culture and transfection

COS-7 and HeLa cells were grown in Dulbecco's modified Eagle's medium (Wako Pure Chemical Industries, Tokyo, Japan) supplemented with 10% FBS, 100 U/ml penicillin, and 100 μ g/ml streptomycin (Wako Pure Chemical Industries). HepG2 cells were grown in Dulbecco's modified Eagle's medium supplemented with 10% FBS, 1% nonessential amino acids (Wako Pure

Chemical Industries), 100 U/ml penicillin, and 100 μ g/ml streptomycin. Jurkat T cells were maintained in 75 cm² flasks in RPMI-1640 medium (Wako Pure Chemical Industries) containing 10%

TABLE 1. Molecular structures of CU-1, CU-2, CU-3, CU-3-1, CU-3-2, CU-3-3, and CU-4

ID	Structure
CU-1	
CU-2	
CU-3	
CU-3-1	
CU-3-2	
CU-3-3	
CU-4	

FBS, 100 U/ml penicillin, and 100 $\mu\text{g/ml}$ streptomycin. The cells were maintained at 37°C in an atmosphere containing 5% CO_2 .

COS-7 cells were seeded in 60 mm dishes at a density of 2.5×10^5 cells/dish. cDNA was transfected into COS-7 cells by electroporation with a Gene Pulser Xcell™ Electroporation System (Bio-Rad Laboratories) according to the manufacturer's instructions.

cDNA constructs

The expression plasmids, p3xFLAG-CMV-pig DGK α (19), -rat DGK β (19), -human DGK γ (19), -human DGK δ 1- Δ SAM (20, 21), -human DGK η 1 (22), -human DGK ϵ (23), -human DGK ζ (24), -human DGK ι (25), -human DGK θ (26) and -human DGK κ (27) were generated as described (18). cDNAs of DGK α - Δ 1-196 and DGK α - Δ 1-332 (28) were amplified by PCR and inserted into p3xFLAG-CMV vector.

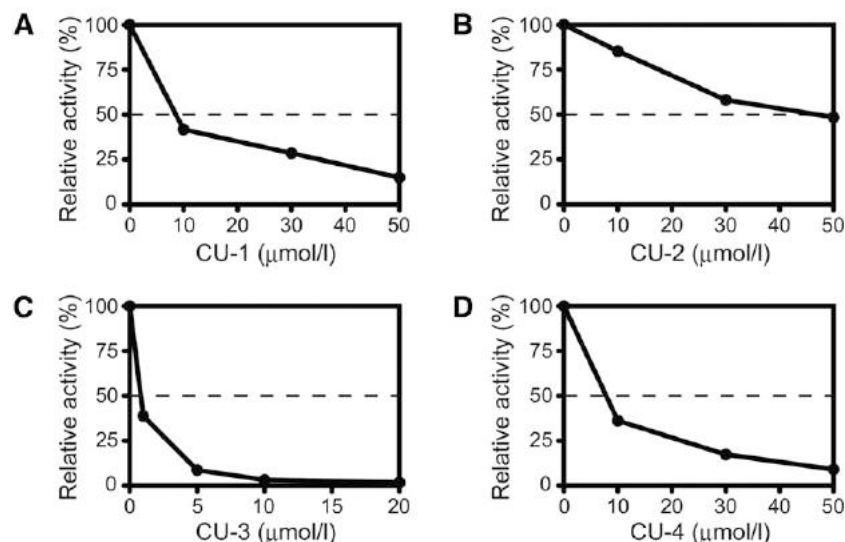
Western blot analysis

COS-7 cell lysates expressing the 3xFLAG tagged proteins were separated on SDS-polyacrylamide gel electrophoresis. The separated proteins were transferred to a polyvinylidene difluoride (PVDF) membrane (Pall Corporation, Tokyo, Japan) and blocked with Block Ace (Dainippon Pharmaceutical, Tokyo, Japan). The membrane was incubated with an anti-FLAG antibody (Sigma-Aldrich, St. Louis, MO) in 10% Block Ace for 1 h. The immunoreactive bands were then visualized using a peroxidase-conjugated anti-mouse IgG antibody (Jackson ImmunoResearch Laboratories) and the Enhanced Chemiluminescence Western Blotting Detection System (GE Healthcare, Tokyo, Japan).

HTS

For HTS, 384-well plates were predisposed with 60 nl (final concentration: 30 or 50 μM) of each compound. Glutathione

Experiment 1



Experiment 2

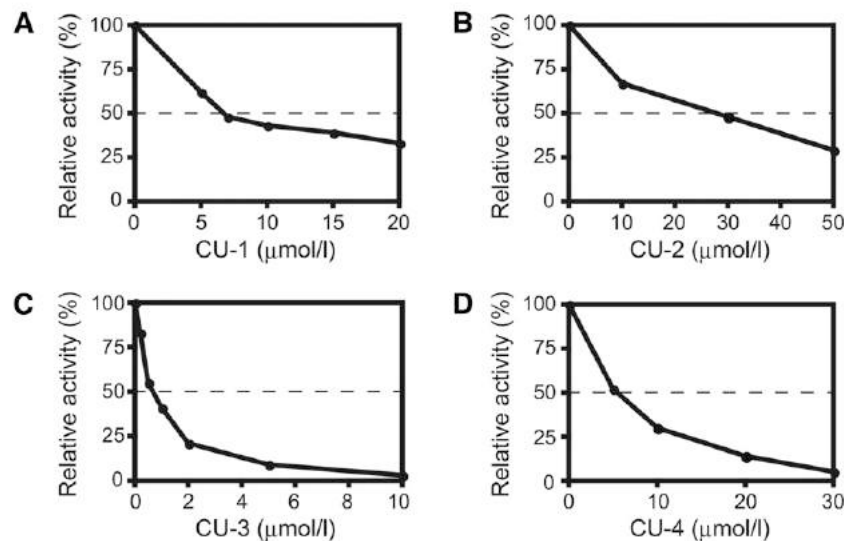


Fig. 1. Effects of CU-1, CU-2, CU-3, and CU-4 on DGK α activity. Purified DGK α (1.25 μg) was incubated with various concentrations of CU-1 (A), CU-2 (B), CU-3 (C), or CU-4 (D) as indicated for 5 min. Values are the average of duplicate determinations, which were within 5% of the mean. Similar results were obtained in two repeated experiments (experiments 1 and 2).

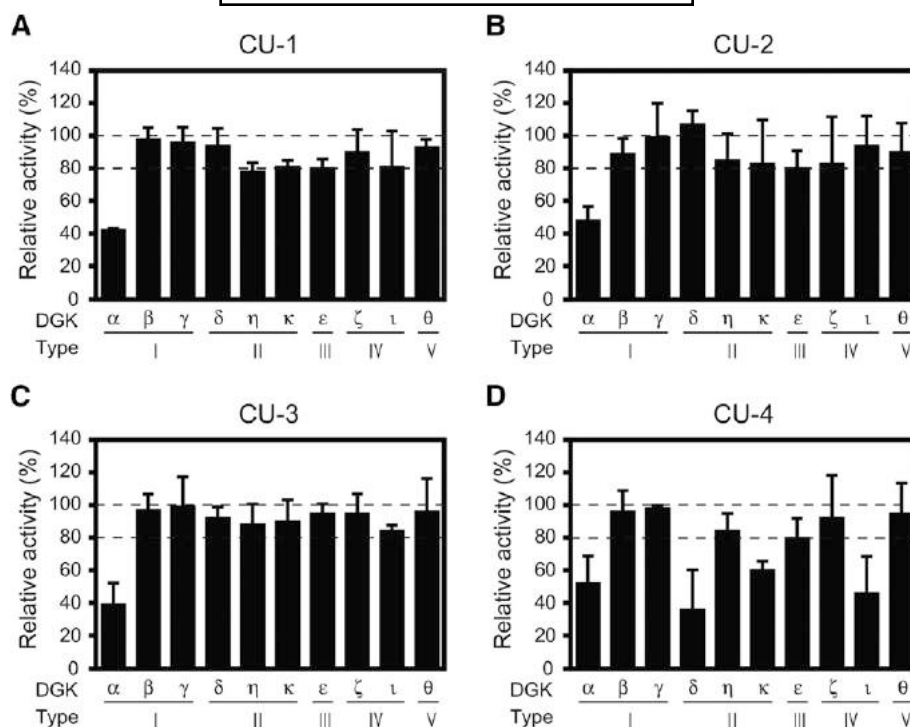


Fig. 2. Effects of CU-1, CU-2, CU-3, and CU-4 on DGK isozyme activities. The 12,000 *g* supernatant (5 μ g) of the extracts from COS-7 cells expressing DGK α , β , γ , δ , η , κ , ϵ , ζ , ι , or θ (A), CU-2 (30 μ M) (B), CU-3 (1 μ M) (C), or CU-4 (5 μ M) (D) as indicated for 5 min. The values in the absence of CU-1, CU-2, CU-3, and CU-4 (supplementary Fig. 1) were set to 100%. * $P < 0.05$, ** $P < 0.01$.

S-transferase-fused pig DGK α was expressed in Sf9 insect cells and purified with a glutathione-Sepharose column (GE Healthcare). The DGK assay was performed using the ADP-Glo™ Kinase Assay Kit (Promega, Tokyo, Japan) at 30°C for 2 h as described previously (18). The chemiluminescence generated in this assay correlates to the amount of ADP generated, which is equivalent to the phosphatidic acid (PA) produced, in the kinase assay, indicating kinase activity. The chemiluminescence was measured using a PHERAstar microplate reader (BMG LABTECH, Offenburg, Germany). The assay performance was consistent across all plates, which was evident due to the robust *Z'* factor.

Chemical compounds

CU-1, -2, -3, and -4 were obtained from Drug Discovery Initiative, University of Tokyo. For further characterization of CU-3 [inhibition mechanisms of CU-3, inhibition effects of CU-3 in cells, induction of apoptosis in cancer cells by CU-3, and enhancement of the interleukin-2 (IL-2) production by CU-3 (see Results)], highly pure CU-3 was resynthesized and supplied by Namiki Shoji (Tokyo, Japan).

Determination of DGK activity in vitro

COS-7 cells (60 mm dish) expressing the various 3xFLAG-tagged DGK isozymes were harvested in lysis buffer (0.5 ml/60 mm dish) containing 50 mM HEPES (pH 7.2), 150 mM NaCl, 5 mM MgCl₂, 1 mM dithiothreitol, 1 mM phenylmethylsulfonyl fluoride, and the Complete Protease Inhibitor mixture (Roche Molecular Biochemicals, Tokyo, Japan). After centrifugation at 400 *g* for 5 min, the resultant supernatant was used for the DGK activity assays.

The octyl glucoside mixed micellar DGK activity assay (29) was modified and performed in a 96-well microplate. The assay mixture (25 μ l) contained 50 mM MOPS (pH 7.4), 50 mM *n*-octyl- β -D-glucoside (Dojindo Laboratories, Kumamoto, Japan), 1 mM dithiothreitol, 100 mM NaCl, 20 mM NaF, 10 mM MgCl₂, 1 μ M

CaCl₂, 10 mM (27 mol%) phosphatidylserine (PS; Sigma-Aldrich), 2 mM (5.4 mol%) 1,2-dioleoyl-*sn*-glycerol (Sigma-Aldrich), 0.2 mM ATP, and 1.25 μ g of purified glutathione *S*-transferase-fused pig DGK α or 2.5 μ g of the COS-7 cell lysates expressing the 3xFLAG-tagged DGK α or other isozymes. We confirmed that the assays were linear with respect to protein concentration and time.

Determination of the DGK activity in cells by LC/MS

Determination of the DGK activity in cells by LC/MS was carried out as described previously (30, 31). COS-7 cells expressing DGK α - Δ 1–196 (a constitutively active mutant) were harvested in phosphate-buffered saline. Total lipids were extracted from the cells according to the method of Bligh and Dyer (32). The extracted cellular lipids (10 μ l) containing 65 pmol of the 28:0-PA internal standard (Sigma-Aldrich) were separated on the LC system (Accela LC Systems, Thermo Fisher Scientific, Tokyo, Japan) using a UK-Silica column (3 μ m, 150 \times 2.0 mm inner diameter; Imtakt, Kyoto, Japan) (30, 31). Mobile phase A consisted of chloroform-methanol-ammonia (89:10:1), and mobile phase B

TABLE 2. Apparent IC₅₀ values of CU-1 and CU-3 against 10 DGK isozymes

DGK isozyme	IC ₅₀ of CU-1 (μ M)	IC ₅₀ of CU-3 (μ M)
α (type I)	8	0.6
β (type I)	43	36
γ (type I)	37	28
δ (type II)	33	36
η (type II)	32	7
κ (type II)	46	32
ϵ (type III)	24	8
ζ (type IV)	47	30
ι (type IV)	27	11
θ (type V)	30	15

consisted of chloroform-methanol-ammonia-water (55:39:1:5). The gradient elution program was as follows: 30% B for 5 min, 30–60% B over 25 min, 60–70% over 10 min, followed by 70% B for 5 min. The flow rate was 0.3 ml/min, and the chromatography was performed at 25°C.

The LC system described above was coupled online to an Exactive Orbitrap MS (Thermo Fisher Scientific) equipped with an ESI source. The ion spray voltage was set to –5 kV and 5 kV in the negative and positive ion mode, respectively. The capillary temperature was set to 300°C. The other parameters were set according to the manufacturer's recommendations. Individual phospholipids were measured by scanning from m/z 450 to 1,100 in the negative or positive ion modes using an Orbitrap Fourier Transform MS with a resolution of 50,000. The MS peaks were identified based on their m/z value and were presented in the form of $X:Y$, where X is the total number of carbon atoms and Y is the total number of double bonds in both acyl chains of the phospholipid.

Apoptosis analysis

HepG2, HeLa, and COS-7 cells were incubated in a 96-well plate in the presence or absence of CU-3 (5 μ M) for 24 h. The caspase-3/7 assay (Caspase-Glo[®] 3/7; Promega) was conducted according to the manufacturer's description. After a 1 h incubation at 25°C, each sample was measured in a microplate reader (GloMax[®]-Multi+ Detection System; Promega).

Assay for IL-2 mRNA expression in Jurkat T cells

The assay for IL-2 mRNA expression in Jurkat T cells was carried out as previously reported (33). Jurkat cells were preincubated in 35 mm culture dishes filled with 2 ml of RPMI in the presence or absence of CU-3 (5 μ M) for 5 min. Concanavalin A (Con A) was then added to the media, and the cells were further incubated for 3 h, collected by centrifugation (400 g, 5 min), and lysed with 1 ml of ISOGEN (Wako Pure Chemical Industries). Total RNA was prepared, and 1 μ g of total RNA was reverse transcribed into cDNA according to the manufacturer's instructions

(for ISOGEN). PCR amplification (34 cycles) was performed using the following primers: 5'-ATGTACAGGATGCAACTCCTGTCTT-3' and 5'-GTT AGTGTGAGATGATGCTTTGAC-3' for IL-2 and 5'-ACCACAGTCCATGCCATCAC-3' and 5'-TCCACACCCTGTTGCTGTA-3' for glyceraldehyde-3-phosphate dehydrogenase. PCR products were then separated by 1% agarose gel electrophoresis and visualized with ethidium bromide. The visualized bands were digitized and quantified using Adobe Photoshop and National Institutes of Health (NIH) Image software.

RNA interference of DGK α

DGK α Stealth select RNAi (catalog number HSS102626; Invitrogen, Tokyo, Japan) was used. Jurkat T cells suspended in un-supplemented, prewarmed RPMI, with 500 nM of human si-DGK α or nontargeting control siRNA (Invitrogen) in 4 mm cuvettes (Nepa Gene) were electroporated at 210 V and 950 microfarads using the GenePulsar Xcell Electroporation System (Bio-Rad Laboratories). After electroporation, cells were incubated for 48 h in culture medium.

Western blot analysis

Lysates of HepG2, HeLa, Jurkat, or COS-7 cells were separated on SDS-polyacrylamide gel electrophoresis. The separated proteins were transferred to a PVDF membrane (Bio-Rad Laboratories) and blocked with Block Ace (Dainippon Pharmaceutical). The membrane was incubated with anti-DGK α (34) antibody in 10% Block Ace for 1 h. The immunoreactive bands were then visualized using a peroxidase-conjugated anti-rabbit IgG antibody (Jackson ImmunoResearch Laboratories) and the Enhanced Chemiluminescence Western Blotting Detection System (GE Healthcare).

RESULTS

Core library screen to identify compounds that inhibit DGK α activity

To identify specific inhibitors for DGK α activity, we screened the Core Library (Drug Discovery Initiative,

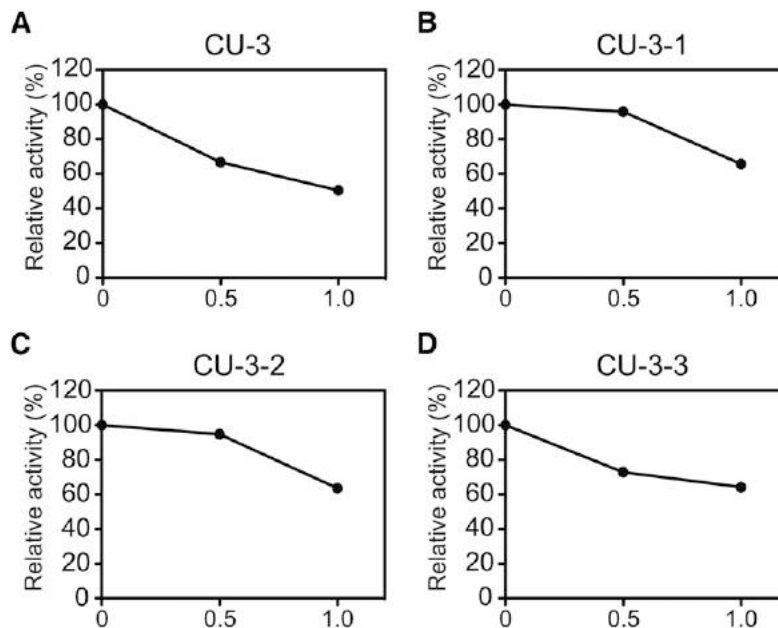


Fig. 3. Effects of CU-3 and its derivatives (CU-3-1, CU-3-2, and CU-3-3) on DGK α activity. The 12,000 g supernatant (5 μ g) of the extracts from COS-7 cells expressing DGK α was incubated for 5 min in the presence or absence (DMSO alone) of CU-3 (A) and its derivatives: CU-3-1 (B), CU-3-2 (C), or CU-3-3 (D). The values in the absence of CU-3, CU-3-1, CU-3-2, and CU-3-3 (supplementary Fig. 2) were set to 100%.

University of Tokyo) that consists of 9,600 compounds using a recently established, simple DGK assay (18). Purified DGK α was incubated with these compounds at a concentration of 30 μ M. We set the threshold for hit compounds at >20% inhibition for all compounds and identified 103 hit compounds. These hit compounds were then subjected to the second screen at a concentration of 50 μ M to assess the reproducibility.

We selected four compounds, CU-1, -2, -3, and -4 (Table 1), that reproducibly and strongly inhibited DGK α activity. Their IC₅₀ values were \sim 8, 27, 0.6, and 6 μ M, respectively (Fig. 1A–D). Doses of 10 μ M and 30 μ M of CU-3 and CU-4, respectively, almost completely inhibited DGK α activity (Fig. 1C, D).

Comparison of the inhibitory activities of CU-1, -2, -3, and -4 against the 10 DGK isozymes

We have already demonstrated that R59022 and R59949 only semiselectively inhibited the 10 DGK isozymes (18). Using the same system, we next compared the inhibitory activities of CU-1, -2, -3, and -4 against all 10 DGK isozymes. As previously reported (18), the expression levels of the DGK isozymes were comparable to each other. The concentrations of these compounds at their approximate IC₅₀ values (10, 30, 1, and 5 μ M, respectively) against DGK α (see Fig. 1) were used. When DGK α activity was inhibited to <50% by CU-1, -2, and -3, at least >75, 80, and 75% activities of the other nine isozymes remained, respectively (Fig. 2A–C); however, in addition to DGK α , CU-4 strongly inhibited the δ -, ϵ -, and ι -isozymes as well (Fig. 2D). These results indicate that CU-1, -2, and -3, but not CU-4, selectively inhibit DGK α .

Among CU-1, -2, and -3, the IC₅₀ value of CU-2 (27 μ M) is relatively high (Fig. 1). Therefore, we focused on CU-1 and -3 and further determined their selectivity for DGK α . The IC₅₀ values of CU-1 and -3 against all 10 DGK isozymes were compared (Table 2). The apparent IC₅₀ values of CU-1 and -3 against the β - to θ -isozymes were 3- to 6-fold and 12- to 60-fold higher than those of DGK α , respectively (Table 2). Therefore, compared with CU-1, CU-3 showed clearly higher selectivity for DGK α . Hence, we selected CU-3 for further analyses.

The effects of the three derivatives (CU-3-1, CU-3-2, and CU-3-3) of CU-3 (Table 1) were examined. Furan in CU-3 is substituted with *N*-methylpyrrole, pyridine, and benzene for CU-3-1, CU-3-2, and CU-3-3, respectively (Table 1). Moreover, although CU-3 has three carbons between 2-thioxo-1,3-thiazolidin-4-one and furan, CU-3-1, CU-3-2, and CU-3-3 have only one carbon between 2-thioxo-1,3-thiazolidin-4-one and *N*-methylpyrrole, pyridine, and benzene (Table 1). As shown in Fig. 3, the inhibitory effect of CU-3 on DGK α activity was stronger than that of CU-3-1, CU-3-2, and CU-3-3, indicating that CU-3 is the strongest DGK α inhibitor among these derivatives.

Inhibition mechanisms of CU-3

We next attempted to reveal the inhibition mechanisms of CU-3. We first examined which region of DGK α was targeted by CU-3. We prepared truncation mutants lacking the recoverin homology domain—the EF-hand motifs

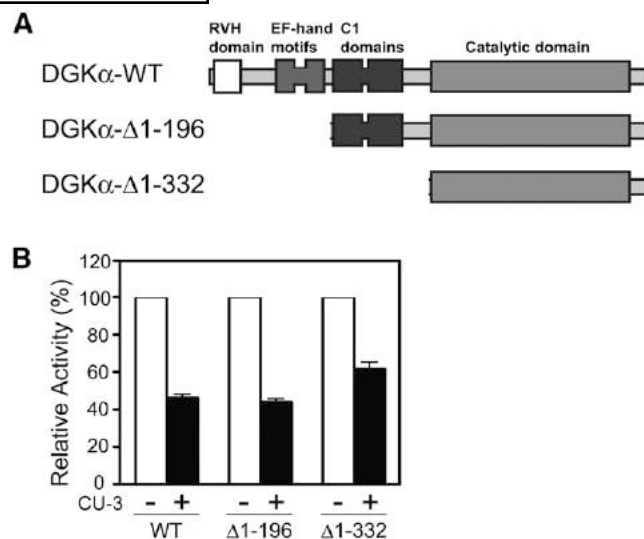


Fig. 4. Effects of CU-3 on the activities of the DGK α truncation mutants. A: Schematic presentation of DGK α truncation mutants. RVH, recoverin homology. B: The 12,000 *g* supernatant (5 μ g) of the extracts from COS-7 cells expressing wild-type DGK α , DGK α - Δ 1-196, or DGK α - Δ 1-332 was incubated for 5 min in the presence (1 μ M) or absence (DMSO alone) of CU-3. The activities of wild-type DGK α , DGK α - Δ 1-196, and DGK α - Δ 1-332 in the absence of CU-3 are defined as 100%.

(DGK α - Δ 1-196) and the recoverin homology domain—the C1 domains (DGK α - Δ 1-332) (Fig. 4A). CU-3 inhibited the DGK activities of the wild-type enzyme and these mutants to a similar extent (Fig. 4B). These results indicate that CU-3 targets the catalytic domain, not the regulatory region, of DGK α . Although DGK α is activated by Ca²⁺ (7, 35), these mutants commonly lack the Ca²⁺ binding EF-hand motifs and show strong Ca²⁺-independent activity (28, 36). Therefore, it is likely that Ca²⁺ is not involved in the inhibition mechanism of CU-3.

It was reported that in addition to wild-type DGK α (35), DGK α - Δ 1-332 (catalytic domain alone) was also activated by PS (28). Therefore, we next determined the EC₅₀ values of PS for DGK α activity in the presence and absence of CU-3. PS strongly activated DGK α , with activation reaching a maximum at \sim 23.0 mol% in the absence of CU-3 (Fig. 5). The apparent EC₅₀ of the isozyme for PS was 12.0 mol% \pm 0.0 (n = 3) in the absence of CU-3 (Fig. 5 and

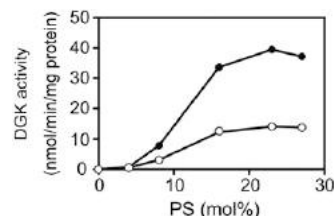


Fig. 5. Effect of CU-3 on the PS dependency of DGK α . The 12,000 *g* supernatant (5 μ g) of the extracts from COS-7 cells expressing DGK α was incubated with various concentrations of PS as indicated for 5 min in the presence (1 μ M, open circle) or absence (DMSO alone, closed circle) of CU-3. The values are the averages of duplicate determinations. The data shown are representative of three separate experiments.

TABLE 3. Apparent EC_{50} values of DGK α for PS in the presence or absence of CU-3

	EC_{50} (mol%)	<i>P</i>
DMSO	12.0 ± 0.0	—
CU-3	13.0 ± 0.6	NS

The values are presented as the mean ± SD (n = 3).

Table 3. The addition of CU-3 did not markedly affect the EC_{50} value of PS (13.0 ± 0.6 mol%, n = 3) (Fig. 5 and Table 3).

We next measured the kinetic parameter for DG. The activity of DGK α increased in a DG dose-dependent manner (Fig. 6A). A double reciprocal plot provided the K_m value for DG in the absence of CU-3 (3.4 ± 1.0 mol%, n = 3; Fig. 6B and Table 4). As shown in Fig. 6B and Table 4, CU-3 did not significantly affect the apparent K_m value for DG (2.9 ± 0.5 mol%, n = 3).

We next determined the kinetic parameter for ATP in the presence and absence of CU-3. The activity of DGK α was increased in an ATP dose-dependent manner (Fig. 7A). A double reciprocal plot provided the apparent K_m value for ATP in the absence of CU-3 (0.25 ± 0.07 mM, n = 3; Fig. 7B and Table 5). However, the K_m value for ATP in the presence of CU-3 was significantly increased to 0.48 ± 0.07 mM, n = 3 (Fig. 6B and Table 5). The V_{max} value was not markedly changed in the presence of CU-3 (Fig. 7B). These results strongly suggest that CU-3 competitively inhibited the affinity of DGK α for ATP.

Inhibition effects of CU-3 in cells

We showed that CU-3 intensely inhibited DGK α activity in vitro (Figs. 1–7). Next, the inhibition effects of

TABLE 4. Apparent K_m values of DGK α for DG in the presence or absence of CU-3

	K_m (mol%)	<i>P</i>
DMSO	3.4 ± 1.0	—
CU-3	2.9 ± 0.5	NS

The values are presented as the mean ± SD (n = 3).

CU-3 on DGK α in cell were determined using our newly established LC/MS method (30, 31). The overexpression of DGK α - Δ 1–196 (Fig. 8A), a constitutively active mutant, clearly increased the total amount of PA (approximately a 15% increase) in COS-7 cells (Fig. 8B). Moreover, the addition of CU-3 significantly reduced the total PA amount that was increased by the overexpression of DGK α - Δ 1–196 (Fig. 8B).

In addition to the total amount of PA (Fig. 8B), the amounts of each PA molecular species were also determined (Fig. 8C). To facilitate comparison, relative changes (p3xFLAG-DGK α - Δ 1–196-transfected cells vs. p3xFLAG vector-transfected cells in the presence or absence of CU-3) were also shown (Fig. 8D). The amounts of broad PA molecular species such as 34:1-, 34:0-, 36:4-, 36:3-, 38:5-, and 38:4-PA were clearly increased by the overexpression of DGK α - Δ 1–196 in COS-7 cells (Fig. 8C, D). Particularly, the amount of 38:4-PA was increased to ~200%. As shown in Fig. 8C, D, CU-3 (2 μ M) significantly inhibited the amounts of the PA molecular species that were increased by the overexpression of DGK α - Δ 1–196, indicating that the inhibitor negatively affected the activity of DGK α in the cells.

Induction of apoptosis in cancer cells by CU-3

We next examined whether CU-3 induces apoptosis in a human hepatocellular carcinoma cell line HepG2

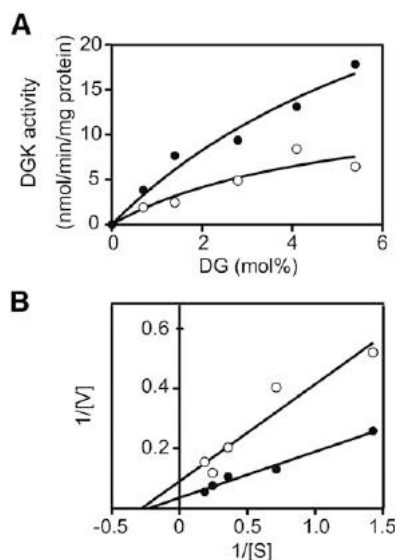


Fig. 6. Effect of CU-3 on the affinity of DGK α for DG. A: The 12,000 *g* supernatant (5 μ g) of the extracts from COS-7 cells expressing DGK α was incubated with various concentrations of DG as indicated for 5 min in the presence (1 μ M, open circle) or absence (DMSO alone, closed circle) of CU-3. B: Lineweaver-Burk plots of the data. The values are the averages of duplicate determinations. The data shown are representative of three separate experiments.

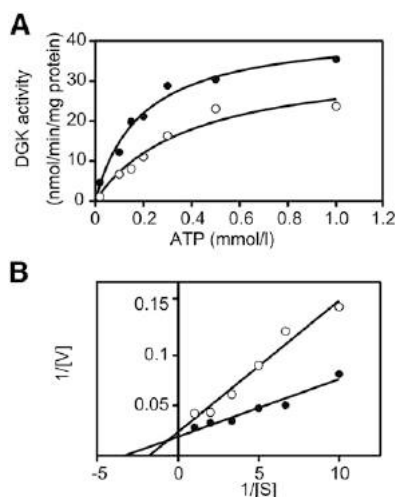


Fig. 7. Effect of CU-3 on the affinity of DGK α for ATP. A: The 12,000 *g* supernatant (5 μ g) of the extracts from COS-7 cells expressing DGK α was incubated with various concentrations of ATP as indicated for 5 min in the presence (1 μ M, open circle) or absence (DMSO alone, closed circle) of CU-3. B: Lineweaver-Burk plots of the data. The values are the averages of duplicate determinations. The data shown are representative of three separate experiments.

TABLE 5. Apparent K_m values of DGK α for ATP in the presence or absence of CU-3

	K_m (mM)	P
DMSO	0.25 \pm 0.07	—
CU-3	0.48 \pm 0.07	0.023

The values are presented as the mean \pm SD (n = 3).

because DGK α was highly expressed in the cell lines (Fig. 9A) and significantly enhanced their cell growth (9). To assess this possibility, caspase-3/7 activity was determined. As shown in Fig. 9B, CU-3 markedly enhanced the caspase-3/7 activity (an \sim 50% increase) of HepG2 cells. Moreover, we utilized HeLa cells (a human cervical carcinoma cell line) because DGK α was highly expressed in the cells (Fig. 9A) and a DGK inhibitor R59022 induced their cell death (37). As shown in Fig. 9C, essentially the same results (an \sim 24% increase of caspase-3/7 activity) were obtained with HeLa cells. However, the caspase-3/7 activity of COS-7 epithelial cells (monkey kidney-derived, noncancerous cell line) was not augmented by CU-3

(Fig. 9D), suggesting that CU-3 is not nonspecifically toxic to cells.

Enhancement of the IL-2 production by CU-3

We next tested whether CU-3 enhanced the function of T cells. To assess this possibility, we determined the Con A-induced IL-2 mRNA production activity of Jurkat cells (a human T-cell line). As shown in Fig. 10, IL-2 mRNA in Jurkat T cells was not detectable in the absence of Con A, and Con A markedly induced the IL-2 mRNA production of the cells. CU-3 further enhanced IL-2 mRNA production activity (an \sim 50% increase) of Jurkat T cells (Fig. 10). These results indicate that CU-3 enhanced the function of T cells.

To demonstrate that CU-3 causes IL-2 production through the inhibition of DGK α , we compared the effects of CU-3 and DGK α -siRNA side by side and examined whether the RNA interference further enhances the effects of the inhibitor. CU-3 and DGK α -siRNA increased IL-2 production to almost the same extents (Fig. 11). Moreover, DGK α -siRNA did not further enhance the

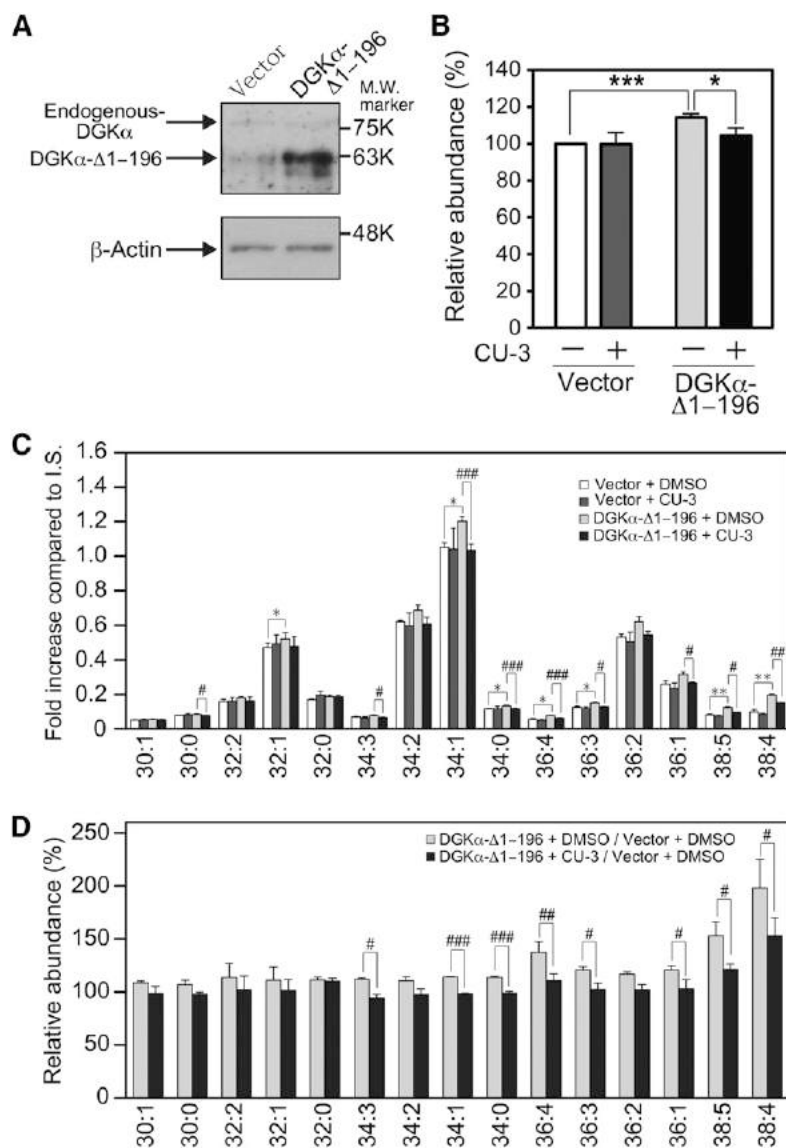


Fig. 8. Effect of CU-3 on the DGK α activity in cells. COS-7 cells were transfected with p3xFLAG-DGK α - Δ 1-196 or p3xFLAG vector alone (Vector). After a 24 h incubation, 2 μ M of CU-3 or DMSO alone was added and further incubated for 24 h. A: Expression of endogenous DGK α and DGK α - Δ 1-196 in COS-7 cells. COS-7 cells transfected with p3xFLAG-CMV vector alone or p3xFLAG-CMV-DGK α - Δ 1-196 were harvested, and the cell lysates (15 μ g of protein) were analyzed by Western blotting using anti-DGK α antibody. B-D: The amounts of the total PAs (B) and major PA molecular species (C) in COS-7 cells were quantified using the LC/MS method. The values are presented as the mean \pm SD (n = 3). B: * P < 0.05, *** P < 0.005. C: * P < 0.05, ** P < 0.01 (p3xFLAG-vector-transfected cells in the absence of CU-3 vs. p3xFLAG-DGK α - Δ 1-196-transfected cells in the absence of CU-3); # P < 0.05, ## P < 0.01, ### P < 0.005 (p3xFLAG-DGK α - Δ 1-196-transfected cells in the absence of CU-3 vs. p3xFLAG-DGK α - Δ 1-196-transfected cells in the presence of CU-3). p3xFLAG-vector-transfected cells in the absence of CU-3, white bars; p3xFLAG-vector-transfected cells in the presence of CU-3, dark gray bars; p3xFLAG-DGK α - Δ 1-196-transfected cells in the absence of CU-3, light gray bars; p3xFLAG-DGK α - Δ 1-196-transfected cells in the presence of CU-3, black bars. (D) The results are presented as the relative value of major PA molecular species of p3xFLAG-DGK α - Δ 1-196-transfected cells versus p3xFLAG vector-transfected cells in the presence (black bars) or absence (white bars) of CU-3. # P < 0.05, ## P < 0.01, ### P < 0.005.

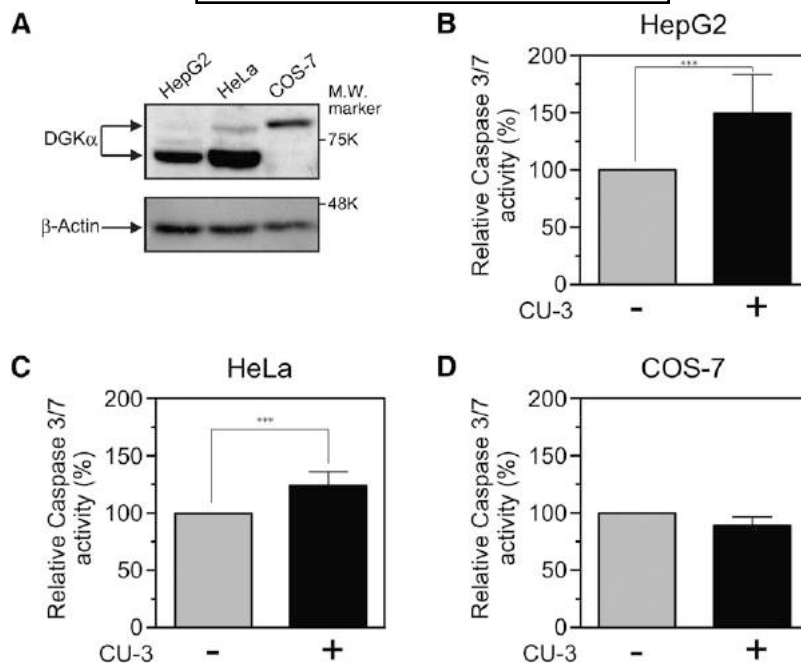


Fig. 9. Effect of CU-3 on the apoptosis of HepG2, HeLa, and COS-7 cells. **A:** Expression of DGK α [80 kDa and 70 kDa (10)] in HepG2, HeLa, and COS-7 cells. HepG2, HeLa, and COS-7 cells were harvested, and the cell lysates (15 μ g of protein) were analyzed by Western blotting using anti-DGK α antibody. **B–D:** After the addition of 5 μ M of CU-3 or DMSO alone, HepG2 (**B**), HeLa (**C**), and COS-7 (**D**) cells were incubated for 24 h. The caspase-3/7 assay was conducted according to the manufacturer's description. After a 1 h incubation at 25°C, each sample was measured in a microplate reader. The values are presented as the mean \pm SD ($n = 6$). *** $P < 0.005$.

effect of CU-3 (Fig. 11), indicating that CU-3 and DGK α -siRNA inhibit the same target, DGK α .

DISCUSSION

We screened a library containing 9,600 compounds using a high-throughput chemiluminescence-based assay that was recently established (18). Among the compounds, CU-3 was identified as a potent and selective inhibitor against the α -isozyme of DGK (Figs. 1 and 2; Table 2). Compared with commercially available DGK inhibitors, R59022 and R59949 (18), CU-3 exhibited higher efficiency and selectivity against DGK α . The IC_{50} value of CU-3 (0.6 μ M) (Fig. 1) was markedly lower than that of R59022 and R59949 (\sim 25 μ M and 18 μ M, respectively) (18). R59022 and R59949 only semiselectively inhibited type I, III, and V DGKs α , ϵ , and θ , and type I and II DGKs α , γ , δ , and κ , respectively (18). Moreover, the K_m value of CU-3 for DGK α was at least \sim 12 times lower than those for other DGK isozymes (Fig. 2 and Table 2). Stemphone, a fungal metabolite, has also been reported to be a DGK inhibitor (38). However, its DGK-isozyme selectivity is not known. Therefore, this study is the first report of a highly α -isozyme selective inhibitor.

DGK α - Δ 1–332 (catalytic domain alone) (Fig. 4A) lacks the regulatory region including the Ca²⁺ binding EF-hand motifs. CU-3 inhibited DGK activities of the full-length enzyme and the mutant to a similar extent (Fig. 4B). The results indicate that the target of CU-3 is the catalytic domain of DGK α . Therefore, it is likely that Ca²⁺ is not involved in the inhibition mechanism of CU-3.

CU-3 did not affect the dependence on an activator PS (Fig. 5 and Table 3). Moreover, CU-3 did not change the K_m value of DGK α for DG (Fig. 6 and Table 4). These results indicate that the affinities for PS and DG failed to be affected by the inhibitor. However, CU-3 significantly decreased the K_m value of DGK α for ATP (Fig. 7 and Table 5). Therefore, it is likely that the inhibitor competitively decreased the affinity for ATP.

CU-3 is not strikingly similar to R59022 (14), R59949 (16), or stemphone (39). CU-3 contains 2-thioxo-1,3-thiazolidin-4-one (Table 1), which is partly similar to ATP. Therefore, it is reasonable to speculate that the inhibitor may partly mimic ATP and eventually decrease the affinity for the substrate of DGK, ATP, as observed in Fig. 7. The primary structures of the catalytic domains of DGK isozymes are highly similar to each other (1–6). Therefore, it is unknown how the isozyme selectivity occurs. To evaluate this issue, a determination of the 3D structure is needed.

In addition to in vitro, CU-3 inhibited cellular DGK α activity in COS-7 cells (Fig. 8). It was noted that a concentration of 2 μ M, which is only \sim 3-fold higher than the IC_{50} value (0.6 μ M) (Fig. 1 and Table 2), strongly inhibited PA production by overexpressed DGK α (Fig. 8). This result suggests that CU-3 has high cell permeability. Therefore, CU-3 is expected to effectively inhibit DGK α in vivo as well.

We demonstrated that CU-3 induced apoptosis in HepG2 hepatocellular carcinoma and HeLa cervical cancer cells (Fig. 9B, C). We also reported that DGK α -specific siRNA attenuated the proliferation of hepatocellular carcinoma (9) and induced apoptosis in melanoma cells (10). Supporting our results, Torres-Ayuso et al. (40) also demonstrated that the growth of colon and breast cancer cell lines was

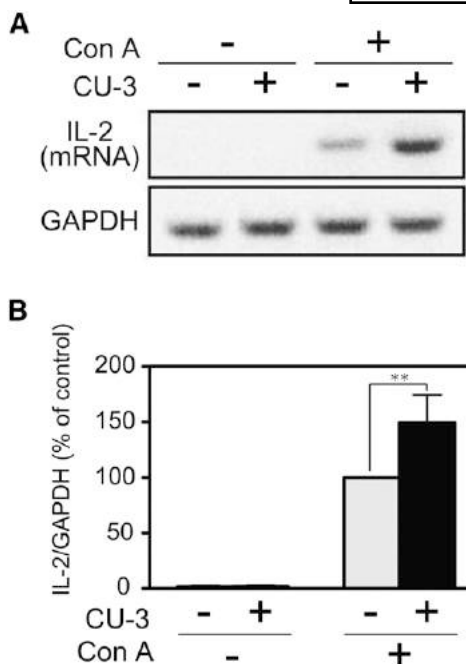


Fig. 10. Effect of CU-3 on the IL-2 production of Jurkat T cells. A: Jurkat T cells were preincubated in 35 mm culture dishes filled with 2 ml RPMI in the presence or absence of CU-3 (5 μ M) for 5 min. Con A was then added to the media, and the cells were further incubated for 3 h. Total RNA was reverse transcribed into cDNA, and PCR amplification (34 cycles) was performed using primers for IL-2 or GAPDH. The PCR products were then separated by agarose gel electrophoresis and visualized with ethidium bromide. The visualized bands were digitized and quantified using Adobe Photoshop and NIH Image software. B: The value in the presence of Con A and in the absence of CU-3 was set to 100%. The values are presented as the mean \pm SD (n = 5). ** $P < 0.01$.

significantly inhibited by DGK α -siRNA and R59949, which attenuates DGK α activity (18). In addition, Dominguez et al. (37) reported that R59022, which most strongly inhibits DGK α (18), negatively affected the proliferation of glioblastoma, melanoma, breast cancer, and cervical cancer cells. It is interesting to investigate the effect of CU-3 on the cell growth of a variety of cancer cells. They also observed that in marked contrast to cancer cells, R59022 did not weaken the growth of noncancerous astrocytes and fibroblasts (37). In this study, we also observed that although CU-3 enhanced the caspase-3/7 activities of HepG2 hepatocellular carcinoma and HeLa cervical cancer cells (Fig. 9B, C), the compound did not increase the caspase-3/7 activity of the noncancer-derived COS-7 cells (Fig. 9D). Therefore, we reproduced their results (37). These findings suggest that cancer-derived cells and noncancer-derived cells may utilize different pathways to induce apoptosis. DGK α seems to be particularly relevant for cancer cells. For example, we have revealed that the expression of DGK α was not detectable in normal hepatocytes, whereas this isozyme was expressed in several hepatocellular carcinoma cell lines (9). Moreover, although normal melanocytes did not express DGK α , several melanoma cell lines did express this isozyme (10). It has been shown that DGK α positively regulated angiogenesis signaling (41). Therefore, it is possible that CU-3 also attenuates the

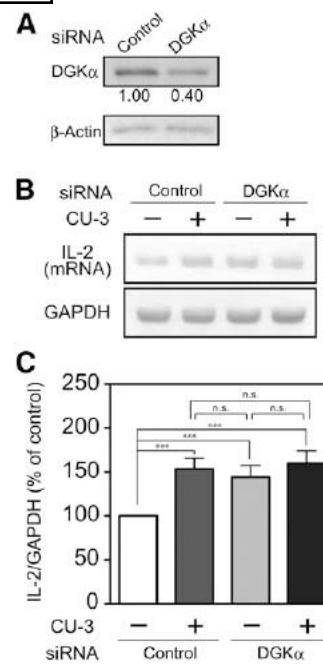



Fig. 11. Effects of DGK α knockdown and CU-3 on IL-2 production of Jurkat T cells. Jurkat T cells were transfected with DGK α -siRNA or nontargeting siRNA (Invitrogen) as indicated. A: After transfection with siRNAs for 48 h, the cells were harvested, and cell lysates (15 μ g of protein) were analyzed by Western blotting with anti-DGK α antibody (upper panel) or anti- β -actin antibody (lower panel). The relative intensity of each band is shown below upper panel. B, C: After transfection with siRNAs for 48 h, the cells were preincubated in the presence or absence of CU-3 (5 μ M) for 5 min. Con A was then added to the media, and the cells were further incubated for 3 h. Total RNA was reverse transcribed into cDNA, and PCR amplification (34 cycles) was performed using primers for IL-2 or GAPDH. The PCR products were then separated by agarose gel electrophoresis and visualized with ethidium bromide. The visualized bands were digitized and quantified using Adobe Photoshop and NIH Image software. The value of control siRNA-treated samples without CU-3 was set to 100%. The values are presented as the mean \pm SD (n = 3). *** $P < 0.005$; n.s., not significant.

angiogenesis of cancer cells in addition to their cell death. It is notable that DGK α -knockout mice are generally healthy, although the mice have a defect in T-cell anergy (12, 13, 42). These results allow us to speculate that DGK α -specific inhibitors would not have severe side effects.

In addition to the induction on cancer cell apoptosis (Fig. 9), the inhibitor promotes IL-2 production (Fig. 10), which is one of the indicators of T-cell activation. Olenchok et al. (12) and Zha et al. (13) previously reported that DGK α is abundantly expressed in T cells, where it facilitates the nonresponsive state, anergy. Thus, the inhibitor of DGK α was expected to enhance T-cell activity. In this study, we found that CU-3 indeed enhanced the IL-2 production of T cells (Fig. 10). Although it has already been reported that the DGK α inhibitor inhibited cancer cell proliferation (37), this study provides a new aspect of the DGK α inhibitor, an enhancer of the immune system. Inactivation (anergy induction) of T cells is the main mechanism for advanced tumors to avoid immune action. Therefore, it is expected that CU-3 is able to activate cancer immunity.

General anticancer drugs attenuate the proliferation and function of both cancer and bone marrow cells (43, 44). Therefore, general anticancer drugs induce not only the attenuation of cancer cell proliferation but also bone marrow suppression/myelosuppression, which is one of the most commonly observed side effects of chemotherapy. Bone marrow suppression results in a decreased number of T cells and, consequently, causes severe side effects, such as recurrent infectious diseases. However, there is no drug that has both protumoral and anti-immunogenic effects. Interestingly, because DGK α has both protumoral and anti-immunogenic properties (4), the DGK α -selective inhibitor CU-3 would simultaneously have antitumoral and proimmunogenic effects. Therefore, CU-3 can be a lead compound to develop an ideal anticancer drug without infectious side effects. Moreover, in addition to the direct effects on apoptosis induction in cancer cells, CU-3 can indirectly induce the death of cancer cells through activation of the immune system. In addition to the development of an anticancer drug, CU-3 will be a great tool for biological science concerning cancer and immunity.

In this study, we were able to obtain DGK isozyme-selective inhibitors, although the 10 DGK isozymes are highly similar to each other. Therefore, our current results encourage us to identify and develop specific inhibitors/activators against every DGK isozyme that can be effective regulators and drugs against a wide variety of physiological events and diseases (4). For example, DGK α : cancer cell growth (9, 10, 37, 40), angiogenesis (41), T-cell proliferation (45), and T-cell anergy (12, 13); DGK β : bipolar disorder (46, 47); DGK γ : actin reorganization (19), allergy (48), and insulin secretion (49); DGK δ : epidermal growth factor receptor signaling (50) and type 2 diabetes (51, 52); DGK η : epidermal growth factor receptor signaling (53), lung cancer (54), bipolar disorder (55, 56), unipolar depression (56), and attention-deficit/hyperactivity disorder (56); DGK κ : hypospadias (57); DGK ϵ : seizure susceptibility/long-term potentiation (58) and Huntington's disease (59); DGK ζ : cell growth (60), T-cell receptor response (61), and brain ischemia (62); DGK ι : Ras signaling (63); and DGK θ : Parkinson's disease (64) and bile acid signaling (65). 

The authors thank Drs. Isabel Merida (Consejo Superior de Investigaciones Científica, Spain) and Andrea Graziani (Università del Piemonte Orientale, Italy) for valuable discussions.

REFERENCES

- Goto, K., Y. Hozumi, and H. Kondo. 2006. Diacylglycerol, phosphatidic acid, and the converting enzyme, diacylglycerol kinase, in the nucleus. *Biochim. Biophys. Acta.* **1761**: 535–541.
- Mérida, I., A. Avila-Flores, and E. Merino. 2008. Diacylglycerol kinases: at the hub of cell signalling. *Biochem. J.* **409**: 1–18.
- Sakane, F., S. Imai, M. Kai, S. Yasuda, and H. Kanoh. 2007. Diacylglycerol kinases: why so many of them? *Biochim. Biophys. Acta.* **1771**: 793–806.
- Sakane, F., S. Imai, M. Kai, S. Yasuda, and H. Kanoh. 2008. Diacylglycerol kinases as emerging potential drug targets for a variety of diseases. *Curr. Drug Targets.* **9**: 626–640.
- Topham, M. K. 2006. Signaling roles of diacylglycerol kinases. *J. Cell. Biochem.* **97**: 474–484.

- van Blitterswijk, W. J., and B. Houssa. 2000. Properties and functions of diacylglycerol kinases. *Cell. Signal.* **12**: 595–605.
- Sakane, F., K. Yamada, H. Kanoh, C. Yokoyama, and T. Tanabe. 1990. Porcine diacylglycerol kinase sequence has zinc finger and E-F hand motifs. *Nature.* **344**: 345–348.
- Schaap, D., J. de Widt, J. van der Wal, J. Vandekerckhove, J. van Damme, D. Gussow, H. L. Ploegh, W. J. van Blitterswijk, and R. L. van der Bend. 1990. Purification, cDNA-cloning and expression of human diacylglycerol kinase. *FEBS Lett.* **275**: 151–158.
- Takeishi, K., A. Taketomi, K. Shirabe, T. Tushima, T. Motomura, T. Ikegami, T. Yoshizumi, F. Sakane, and Y. Maehara. 2012. Diacylglycerol kinase alpha enhances hepatocellular carcinoma progression by activation of Ras-Raf-MEK-ERK pathway. *J. Hepatol.* **57**: 77–83.
- Yanagisawa, K., S. Yasuda, M. Kai, S. Imai, K. Yamada, T. Yamashita, K. Jimbow, H. Kanoh, and F. Sakane. 2007. Diacylglycerol kinase α suppresses tumor necrosis factor- α -induced apoptosis of human melanoma cells through NF- κ B activation. *Biochim. Biophys. Acta.* **1771**: 462–474.
- Kai, M., S. Yasuda, S. Imai, M. Toyota, H. Kanoh, and F. Sakane. 2009. Diacylglycerol kinase α enhances protein kinase C ζ -dependent phosphorylation at Ser311 of p65/RelA subunit of nuclear factor- κ B. *FEBS Lett.* **583**: 3265–3268.
- Olenchock, B. A., R. Guo, J. H. Carpenter, M. Jordan, M. K. Topham, G. A. Koretzky, and X. P. Zhong. 2006. Disruption of diacylglycerol metabolism impairs the induction of T cell anergy. *Nat. Immunol.* **7**: 1174–1181.
- Zha, Y., R. Marks, A. W. Ho, A. C. Peterson, S. Janardhan, I. Brown, K. Praveen, S. Stang, J. C. Stone, and T. F. Gajewski. 2006. T cell anergy is reversed by active Ras and is regulated by diacylglycerol kinase- α . *Nat. Immunol.* **7**: 1166–1173.
- de Chaffoy de Courcelles, D. C., P. Roevens, and H. Van Belle. 1985. R 59 022, a diacylglycerol kinase inhibitor. Its effect on diacylglycerol and thrombin-induced C kinase activation in the intact platelet. *J. Biol. Chem.* **260**: 15762–15770.
- Sakane, F., K. Yamada, and H. Kanoh. 1989. Different effects of sphingosine, R59022 and anionic amphiphiles on two diacylglycerol kinase isozymes purified from porcine thymus cytosol. *FEBS Lett.* **255**: 409–413.
- de Chaffoy de Courcelles, D., P. Roevens, H. Van Belle, L. Kennis, Y. Somers, and F. De Clerck. 1989. The role of endogenously formed diacylglycerol in the propagation and termination of platelet activation. A biochemical and functional analysis using the novel diacylglycerol kinase inhibitor, R 59 949. *J. Biol. Chem.* **264**: 3274–3285.
- Jiang, Y., F. Sakane, H. Kanoh, and J. P. Walsh. 2000. Selectivity of the diacylglycerol kinase inhibitor 3-[2-(4-[bis-(4-fluorophenyl)methylene]-1-piperidinyl)ethyl]-2, 3-dihydro-2-thioxo-4(1H)quinazolinone (R59949) among diacylglycerol kinase subtypes. *Biochem. Pharmacol.* **59**: 763–772.
- Sato, M., K. Liu, S. Sasaki, N. Kunii, H. Sakai, H. Mizuno, H. Saga, and F. Sakane. 2013. Evaluations of the selectivities of the diacylglycerol kinase inhibitors R59022 and R59949 among diacylglycerol kinase isozymes using a new non-radioactive assay method. *Pharmacology.* **92**: 99–107.
- Tsushima, S., M. Kai, K. Yamada, S. Imai, K. Houkin, H. Kanoh, and F. Sakane. 2004. Diacylglycerol kinase γ serves as an upstream suppressor of Rac1 and lamellipodium formation. *J. Biol. Chem.* **279**: 28603–28613.
- Imai, S., F. Sakane, and H. Kanoh. 2002. Phorbol ester-regulated oligomerization of diacylglycerol kinase δ linked to its phosphorylation and translocation. *J. Biol. Chem.* **277**: 35323–35332.
- Sakane, F., S. Imai, K. Yamada, T. Murakami, S. Tsushima, and H. Kanoh. 2002. Alternative splicing of the human diacylglycerol kinase δ gene generates two isoforms differing in their expression patterns and in regulatory functions. *J. Biol. Chem.* **277**: 43519–43526.
- Murakami, T., F. Sakane, S. Imai, K. Houkin, and H. Kanoh. 2003. Identification and characterization of two splice variants of human diacylglycerol kinase η . *J. Biol. Chem.* **278**: 34364–34372.
- Tang, W., M. Bunting, G. A. Zimmerman, T. M. McIntyre, and S. M. Prescott. 1996. Molecular cloning of a novel human diacylglycerol kinase highly selective for arachidonate-containing substrates. *J. Biol. Chem.* **271**: 10237–10241.
- Bunting, M., W. Tang, G. A. Zimmerman, T. M. McIntyre, and S. M. Prescott. 1996. Molecular cloning and characterization of a novel human diacylglycerol kinase ζ . *J. Biol. Chem.* **271**: 10230–10236.
- Ding, L., E. Traer, T. M. McIntyre, G. A. Zimmerman, and S. M. Prescott. 1998. The cloning and characterization of a novel human diacylglycerol kinase, DGK ι . *J. Biol. Chem.* **273**: 32746–32752.

26. Houssa, B., D. Schaap, J. van der Val, K. Goto, H. Kondo, A. Yamakawa, M. Shibata, T. Takenawa, and W. J. van Blitterswijk. 1997. Cloning of a novel human diacylglycerol kinase (DGK θ) containing three cysteine-rich domains, a proline-rich Region, and a pleckstrin homology domain with an overlapping Ras-associating domain. *J. Biol. Chem.* **272**: 10422–10428.
27. Imai, S., M. Kai, S. Yasuda, H. Kanoh, and F. Sakane. 2005. Identification and characterization of a novel human type II diacylglycerol kinase, DGK κ . *J. Biol. Chem.* **280**: 39870–39881.
28. Sakane, F., M. Kai, I. Wada, S. Imai, and H. Kanoh. 1996. The C-terminal part of diacylglycerol kinase α lacking zinc fingers serves as a catalytic domain. *Biochem. J.* **318**: 583–590.
29. Sakane, F., S. Imai, M. Kai, I. Wada, and H. Kanoh. 1996. Molecular cloning of a novel diacylglycerol kinase isozyme with a pleckstrin homology domain and a C-terminal tail similar to those of the EPH family of protein tyrosine kinase. *J. Biol. Chem.* **271**: 8394–8401.
30. Mizuno, S., H. Sakai, M. Saito, S. Kado, and F. Sakane. 2012. Diacylglycerol kinase-dependent formation of phosphatidic acid molecular species during interleukin-2 activation in CTL-2 T-lymphocytes. *FEBS Open Bio.* **2**: 267–272.
31. Sakai, H., S. Kado, A. Taketomi, and F. Sakane. 2014. Diacylglycerol kinase δ phosphorylates phosphatidylcholine-specific phospholipase C-dependent, palmitic acid-containing diacylglycerol species in response to high glucose levels. *J. Biol. Chem.* **289**: 26607–26617.
32. Bligh, E. G., and W. J. Dyer. 1959. A rapid method of total lipid extraction and purification. *Can. J. Biochem. Physiol.* **37**: 911–917.
33. Tanaka, S., E. Akaishi, K. Hosaka, S. Okamura, and Y. Kubohara. 2005. Zinc ions suppress mitogen-activated interleukin-2 production in Jurkat cells. *Biochem. Biophys. Res. Commun.* **335**: 162–167.
34. Yamada, K., F. Sakane, and H. Kanoh. 1989. Immunodetection of 80 kDa diacylglycerol kinase in pig and human lymphocytes and several other cells. *FEBS Lett.* **244**: 402–406.
35. Sakane, F., K. Yamada, S. Imai, and H. Kanoh. 1991. Porcine 80-kDa diacylglycerol kinase is a calcium-binding and calcium/phospholipid-dependent enzyme and undergoes calcium-dependent translocation. *J. Biol. Chem.* **266**: 7096–7100.
36. Sakane, F., S. Imai, K. Yamada, and H. Kanoh. 1991. The regulatory role of EF-hand motifs of pig 80K diacylglycerol kinase as assessed using truncation and deletion mutants. *Biochem. Biophys. Res. Commun.* **181**: 1015–1021.
37. Dominguez, C. L., D. H. Floyd, A. Xiao, G. R. Mullins, B. A. Kefas, W. Xin, M. N. Yacur, R. Abounader, J. K. Lee, G. M. Wilson, et al. 2013. Diacylglycerol kinase α is a critical signaling node and novel therapeutic target in glioblastoma and other cancers. *Cancer Discov.* **3**: 782–797.
38. Nobe, K., M. Miyatake, H. Nobe, Y. Sakai, J. Takashima, and K. Momose. 2004. Novel diacylglycerol kinase inhibitor selectively suppressed an U46619-induced enhancement of mouse portal vein contraction under high glucose conditions. *Br. J. Pharmacol.* **143**: 166–178.
39. Huber, C. S. 1975. The structure of stemphone, a yellow fungal metabolite. *Acta Crystallogr. B.* **31**: 108–113.
40. Torres-Ayuso, P., M. Daza-Martín, J. Martín-Pérez, A. Avila-Flores, and I. Merida. 2014. Diacylglycerol kinase α promotes 3D cancer cell growth and limits drug sensitivity through functional interaction with Src. *Oncotarget.* **5**: 9710–9726.
41. Baldanzi, G., S. Mitola, S. Cutrupi, N. Filigheddu, W. J. van Blitterswijk, F. Sinigaglia, F. Bussolino, and A. Graziani. 2004. Activation of diacylglycerol kinase α is required for VEGF-induced angiogenic signaling in vitro. *Oncogene.* **23**: 4828–4838.
42. Guo, R., C. K. Wan, J. H. Carpenter, T. Mousallem, R. M. Boustany, C. T. Kuan, A. W. Burks, and X. P. Zhong. 2008. Synergistic control of T cell development and tumor suppression by diacylglycerol kinase α and ζ . *Proc. Natl. Acad. Sci. USA.* **105**: 11909–11914.
43. Chabner, B. A., and T. G. Roberts, Jr. 2005. Timeline: chemotherapy and the war on cancer. *Nat. Rev. Cancer.* **5**: 65–72.
44. Pérez-Herrero, E., and A. Fernández-Medarde. 2015. Advanced targeted therapies in cancer: drug nanocarriers, the future of chemotherapy. *Eur. J. Pharm. Biopharm.* **93**: 52–79.
45. Jones, D. R., I. Flores, E. Diaz, C. Martínez-A, and I. Merida. 1998. Interleukin-2 stimulates a late increase in phosphatidic acid production in the absence of phospholipase D activation. *FEBS Lett.* **433**: 23–27.
46. Kakefuda, K., A. Oyagi, M. Ishisaka, K. Tsuruma, M. Shimazawa, K. Yokota, Y. Shirai, K. Horie, N. Saito, J. Takeda, et al. 2010. Diacylglycerol kinase β knockout mice exhibit lithium-sensitive behavioral abnormalities. *PLoS One.* **5**: e13447.
47. Shirai, Y., T. Kouzuki, K. Kakefuda, S. Moriguchi, A. Oyagi, K. Horie, S. Y. Morita, M. Shimazawa, K. Fukunaga, J. Takeda, et al. 2010. Essential role of neuron-enriched diacylglycerol kinase (DGK), DGK β in neurite spine formation, contributing to cognitive function. *PLoS One.* **5**: e11602.
48. Sakuma, M., Y. Shirai, T. Ueyama, and N. Saito. 2014. Diacylglycerol kinase gamma regulates antigen-induced mast cell degranulation by mediating Ca(2+) influxes. *Biochem. Biophys. Res. Commun.* **445**: 340–345.
49. Kurohane Kaneko, Y., Y. Kobayashi, K. Motoki, K. Nakata, S. Miyagawa, M. Yamamoto, D. Hayashi, Y. Shirai, F. Sakane, and T. Ishikawa. 2013. Depression of type I diacylglycerol kinases in pancreatic β -cells from male mice results in impaired insulin secretion. *Endocrinology.* **154**: 4089–4098.
50. Crotty, T., J. Cai, F. Sakane, A. Taketomi, S. M. Prescott, and M. K. Topham. 2006. Diacylglycerol kinase δ regulates protein kinase C and epidermal growth factor receptor signaling. *Proc. Natl. Acad. Sci. USA.* **103**: 15485–15490.
51. Chibalin, A. V., Y. Leng, E. Vieira, A. Krook, M. Bjornholm, Y. C. Long, O. Kotova, Z. Zhong, F. Sakane, T. Steiler, et al. 2008. Downregulation of diacylglycerol kinase delta contributes to hyperglycemia-induced insulin resistance. *Cell.* **132**: 375–386.
52. Miele, C., F. Paturzo, R. Teperino, F. Sakane, F. Formi, F. Oriente, P. Ungaro, R. Valentino, F. Beguinot, and P. Formisano. 2007. Glucose regulates diacylglycerol intracellular levels and protein kinase C activity by modulating diacylglycerol-kinase subcellular localization. *J. Biol. Chem.* **282**: 31835–31843.
53. Yasuda, S., M. Kai, S. Imai, K. Takeishi, A. Taketomi, M. Toyota, H. Kanoh, and F. Sakane. 2009. Diacylglycerol kinase η augments C-Raf activity and B-Raf/C-Raf heterodimerization. *J. Biol. Chem.* **284**: 29559–29570.
54. Nakano, T., A. Irvani, M. Kim, Y. Hozumi, M. Lohse, E. Reichert, T. M. Crotty, D. M. Stafforini, and M. K. Topham. 2014. Diacylglycerol kinase eta modulates oncogenic properties of lung cancer cells. *Clin. Transl. Oncol.* **16**: 29–35.
55. Baum, A. E., N. Akula, M. Cabanero, I. Cardona, W. Corona, B. Klemens, T. G. Schulze, S. Cichon, M. Rietschel, M. M. Nothen, et al. 2008. A genome-wide association study implicates diacylglycerol kinase eta (DGKH) and several other genes in the etiology of bipolar disorder. *Mol. Psychiatry.* **13**: 197–207.
56. Weber, H., S. Kittel-Schneider, A. Gessner, K. Domschke, M. Neuner, C. P. Jacob, H. N. Buttenschon, A. Boreatti-Hummer, J. Volkert, S. Herterich, et al. 2011. Cross-disorder analysis of bipolar risk genes: further evidence of DGKH as a risk gene for bipolar disorder, but also unipolar depression and adult ADHD. *Neuropsychopharmacology.* **36**: 2076–2085.
57. van der Zanden, L. F., I. A. van Rooij, W. F. Feitz, J. Knight, A. R. Donders, K. Y. Renkema, E. M. Bongers, S. H. Vermeulen, L. A. Kiemeny, J. A. Veltman, et al. 2011. Common variants in DGKK are strongly associated with risk of hypospadias. *Nat. Genet.* **43**: 48–50.
58. Rodriguez de Turco, E. B., W. Tang, M. K. Topham, F. Sakane, V. L. Marcheselli, C. Chen, A. Taketomi, S. M. Prescott, and N. G. Bazan. 2001. Diacylglycerol kinase ϵ regulates seizure susceptibility and long-term potentiation through arachidonoyl-inositol lipid signaling. *Proc. Natl. Acad. Sci. USA.* **98**: 4740–4745.
59. Zhang, N., B. Li, I. Al-Ramahi, X. Cong, J. M. Held, E. Kim, J. Botas, B. W. Gibson, and L. M. Ellerby. 2012. Inhibition of lipid signaling enzyme diacylglycerol kinase ϵ attenuates mutant huntingtin toxicity. *J. Biol. Chem.* **287**: 21204–21213.
60. Topham, M. K., M. Bunting, G. A. Zimmerman, T. M. McIntyre, P. J. Blakeshear, and S. M. Prescott. 1998. Protein kinase C regulates the nuclear localization of diacylglycerol kinase-zeta. *Nature.* **394**: 697–700.
61. Zhong, X. P., E. A. Hainey, B. A. Olenchok, M. S. Jordan, J. S. Maltzman, K. E. Nichols, H. Shen, and G. A. Koretzky. 2003. Enhanced T cell responses due to diacylglycerol kinase ζ deficiency. *Nat. Immunol.* **4**: 882–890.
62. Nakano, T., Y. Hozumi, H. Ali, S. Saino-Saito, H. Kamii, S. Sato, T. Kayama, M. Watanabe, H. Kondo, and K. Goto. 2006. Diacylglycerol kinase zeta is involved in the process of cerebral infarction. *Eur. J. Neurosci.* **23**: 1427–1435.
63. Regier, D. S., J. Higbee, K. M. Lund, F. Sakane, S. M. Prescott, and M. K. Topham. 2005. Diacylglycerol kinase ι regulates Ras guanyl-releasing protein 3 and inhibits Rap1 signaling. *Proc. Natl. Acad. Sci. USA.* **102**: 7595–7600.
64. Pankratz, N., J. B. Wilk, J. C. Latourelle, A. L. DeStefano, C. Halter, E. W. Pugh, K. F. Doheny, J. F. Gusella, W. C. Nichols, T. Foroud, et al. 2009. Genomewide association study for susceptibility genes contributing to familial Parkinson disease. *Hum. Genet.* **124**: 593–605.
65. Cai, X., and M. B. Sewer. 2013. Diacylglycerol kinase θ couples farnesoid X receptor-dependent bile acid signalling to Akt activation and glucose homeostasis in hepatocytes. *Biochem. J.* **454**: 267–274.